Group-Size Regulation in Self-organized Aggregation in Robot Swarms

FIRAT, Ziya; Ferrante, Eliseo; Zakir, Raina; JUDHI PRASETYO, X; Tuci, Elio

Published in:
Swarm Intelligence - 12th International Conference, ANTS 2020, Proceedings

DOI:
10.1007/978-3-030-60376-2_26

Publication date:
2020

Document Version
Peer reviewed version

Group-size Regulation in Self-organised Aggregation via Informed Individuals in Robot Swarms

Ziya Firat[1], Eliseo Ferrante[2], Raina Zakir[2], Judhi Prasetyo[1,3], Elio Tuci[1]

[1] Department of Computer Science, University of Namur, Namur, Belgium
ziya.firat@student.unamur.be,elio.tuci@unamur.be
[2] Vrije Universiteit Amsterdam, Amsterdam, The Netherlands e.ferrante@vu.nl
[3] Middlesex University Dubai, Dubai, United Arab Emirates j.prasetyo@mdx.ac.ae

Abstract. In swarm robotics, self-organised aggregation refers to a collective process in which robots form a single aggregate in an arbitrarily chosen aggregation site among those available in the environment, or just in an arbitrarily chosen location. Instead of focusing exclusively on the formation of a single aggregate, in this study we discuss how to design a swarm of robots capable of generating aggregation dynamics that can correspond to a variety of final distributions of the robots to the available aggregation sites. We focus on an environment with two possible aggregation sites, A and B. Our study is based on the working hypothesis that robots distribute on site A and B in quantities that reflect the relative proportion of robots in the swarm that selectively avoid A with respect to those that selectively avoid B, with an as minimal as possible proportion of robots in the swarm that selectively avoid one or the other site. We illustrate the individual mechanisms designed to implement the above mentioned working hypothesis, and we discuss the promising results of a set of simulations that systematically consider a variety of experimental conditions. The results with simulated robots are validate with physical kilobot robots.

1 Introduction

Swarm robotics studied the design of collective behaviours able to tackle task in large and unpredictable environments [1]. Swarm robotics takes inspiration from studies in social insect and other social animals, whereby simple individuals are able to exhibit superior collective intelligence when working in groups [2]. The overall goal is to design systems that are robust, scalable, and flexible like their natural counterparts [1]. To achieve this, swarm robotics relies on the application of the following principles: i) absence of external infrastructure and reliance on only on-board sensing and computation; ii) use of local perception and communication only; that is, each robot can sense and communicate only within a given range via on-board devices; iii) the process of self-organization, that yields from microscopic behaviours and individual interactions to macroscopic complex collective behaviours.

Collective decision-making is the the ability to make a collective decisions only via local interaction and communication [3]. This is an important collective response which has been extensively studied in swarm robotics. Collective decision making can take several forms: it can either be studied explicitly [3, 4] or implicitly in other collective behaviours such as collective motion (decision on a common direction of motion), and aggregation (decision on a common location for gathering in the environment). Two factors that can synergistically or antagonistically influence collective decision-making process are asymmetries in the environment, or the active modulation performed by the all or some of the swarm members [3]. In a seminal study on collective decision making [5], the authors studied collective motion models in presence of so called *implicit leaders* or *informed individuals*. These have a preferred direction of motion to guide collective motion in that direction. The rest of the swarm do not possess a preferred direction of motion, nor is able to recognise informed individuals. The main result of the paper is that even a minority of informed individuals is able to guide the swarm in the desired direction, and that larger groups require smaller proportion of informed individuals for equal levels of accuracy.

As in Couzin's work, also in swarm robotics the framework of informed individuals has been studied mainly in the context of collective motion [6–8]. Recently, this framework has been ported to another collective behaviour, namely self-organized aggregation [9–11]. Self-organised aggregation [12–14] has roots in the biological study of cockroaches [15, 16], where probabilistic models have been proposed. The same models have been adapted and implemented on distributed robotic systems [17, 18, 13]. Besides being another example of collective decision-making, aggregation is a basic building block for other cooperative behaviours [19, 20]. Self-organised aggregation can take place in environments that are completely homogeneous (except for boundaries and potential obstacles) where no perceivable special locations, called sites or shelters, are present, thus robots are required to aggregate anywhere in this environment [21]. Alternatively, as it is the case of the current paper, the sites where robots are required to aggregate can be specific areas in the environment that can be clearly perceived by all or some of the robots [22, 23].

In this paper our objective is to go one step beyond the state of the art to further study how the framework of *informed* robots can be used as guiding principle for self-organization. We build upon recent studies on self-organized aggregation with *informed* robots [9–11], where robots need to select only one site among n possible alternatives, driven by *informed* robots. Each *informed* robot has knowledge on a specific aggregation site to stop on and avoids other aggregation sites. *Non-informed* robots do not possess this information, therefore may potentially aggregate on any side. Additionally, *informed* robots are assumed to be perceivable, through sensing, by other robots (e.g., they emit a signal), while *non-informed* robots cannot be sensed at all. Differently from [9–11], in this paper robots are required to aggregate on both sites according to different proportions as set by the designer. To control the proportion of robots aggregating on the two sides, we design a novel aggregation method. *Informed* robots are

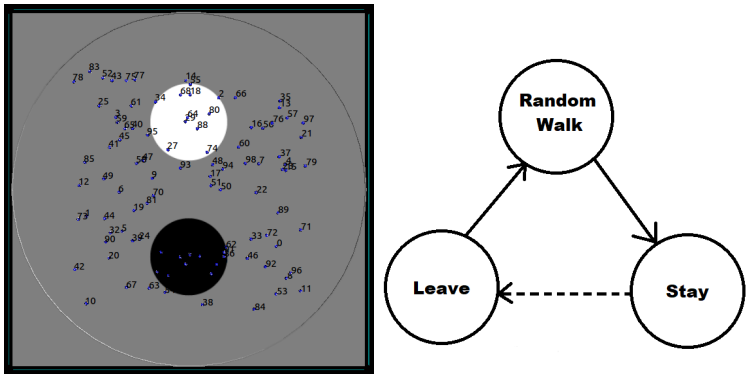

(a) (b)

Fig. 1. (a) The simulated robots' arena with the black and white aggregation site. (b) State diagram of the robots' controller. The dashed line indicates probabilistic transition, the continuous lines indicate non probabilistic transition.

divided in two types, each preferring one of the two sites over the other. To control the relative group size on the two sites, the proposed method only requires the presence of *informed* robots with internal sub-proportions correlating with desired global allocation for the whole swarm. We perform our study using both simulation and real-robot experiments. In simulation we considered a scenarios in a circular arena where the two aggregation sites are represented by black or white colored circles, respectively. Additionally, we also implement our method on a swarm of real kilobots, whereby we used robot themselves as beacons to indicate the two sites because of the sensing limitation of the robot platform, and we developed and used an IR platform, that can be sensed by the kilobots, in order to implement the boundaries of the arena and let kilobots avoid the wall. The results of our simulations and physical robots show interesting relationships between swarm size and sub-proportion of informed agents, both on quality and speed of convergence on the desired aggregation site. In the following sections, we detailed the methods of our study; we discuss the significance of our results for the swarm robotics community, and we point to interesting future directions of work.

2 The simulation environment

A swarm of robots is randomly placed in a circular area with the floor coloured in grey except for two circular aggregation sites, one in which the floor is coloured in white and one in which is black (see Figure 1a). The task of the robots is to form aggregates on both sites according to rules that prescribe which proportion of the swarm has to aggregate on the white site and which proportion on the black site. Each simulated robot is controlled by a probabilistic finite state machine (PFSM,

see also Figure 1b), similar to the one employed in [16, 14, 12, 24]. The robots' controller is made of three states: Random Walk ($\mathcal{RW}$), Stay ($\mathcal{S}$), and Leave ($\mathcal{L}$). When in state $\mathcal{RW}$, the movement of the robot is characterised by an isotropic random walk, with a fixed step length (5 seconds, at 10 cm/s), and turning angles chosen from a wrapped Cauchy probability distribution characterised by the following PDF [25]:

$$f_\omega(\theta, \mu, \rho) = \frac{1}{2\pi} \frac{1-\rho^2}{1+\rho^2-2\rho\cos(\theta-\mu)},\ 0<\rho<1, \tag{1}$$

where $\mu = 0$ is the average value of the distribution, and ρ determines the distribution skewness. For $\rho = 0$ the distribution becomes uniform and provides no correlation between consecutive movements, while for $\rho = 1$ a Dirac distribution is obtained, corresponding to straight-line motion. In this study $\rho = 0.5$. Any robot in state $\mathcal{RW}$ is continuously performing an obstacle avoidance behaviour. To perform obstacle avoidance, first the robot stops, and then it changes its headings of a randomly chosen angle uniformly drawn in $[-\pi, \pi]$ until no obstacles are perceived in the forward direction of motion. Negative angles refer to clockwise rotations, while positive to anticlockwise rotations.

In our model, we consider two type of robots: *informed* robots and *non-informed* robots. *Informed* robots systematically rest only on one site. Some of them, avoid the black site and rest only on the white site (*informed* robots for white); others avoid the white site and rest only on the black site (*informed* robots for black). *Non-informed* robots can potentially rest on both types of site. Note that, the working hypothesis of this study is that the way in which the swarm distributes among the two aggregation sites reflects the relative proportion of *informed* robots for black and for white. For example, if 50% of the *informed* robots are for black and 50% of them are for white, the swarm should generate two equal size aggregates one on the black and one on the white site. This experimental work aims at verifying this working hypothesis by systematically varying the proportion of *informed* robots within the swarm. Moreover, for each proportion of *informed* robots, we vary the relative proportion of *informed* robots for black and for white.

A *non-informed* robot systematically transits from state $\mathcal{RW}$ to state $\mathcal{S}$ anytime it reaches an aggregation site. *Informed* robots for black undergo the same state change only when they reach the black site, thus ignoring the white site. *Informed* robots for white systematically transits from state $\mathcal{RW}$ to state $\mathcal{S}$ anytime they reach a white aggregation site, thus ignoring the black site. For all types of robots, the transaction from the random walk to resting on a site happens in the following: the robots moves forward within the site for a limited number of time steps in order to avoid stopping at the border of the site thus creating barriers preventing the entrance to other robots. Then, they transitions from state $\mathcal{RW}$ to state $\mathcal{S}$.

The robots leave state $\mathcal{S}$ to join state $\mathcal{L}$ with a probability P_{leave}, which is computed in the following:

$$P_{leave} = \begin{cases} e^{-a(k-|n-x|)}, & \text{if } n > 0; \text{ it applies to all types of robots;} \\ 1, & \text{if } n = 0; \text{ only for } \textit{non-informed} \text{ robot;} \end{cases} \quad (2)$$

with $a = 2.0$ and $k = 18$. n is current number of *informed* robots perceived at the site, and x is the number of *informed* robots perceived at the site at the time of joining a site. Note that, for any robots n and x are local estimates based the number of *informed* robots in the perceivable neighborhood which is smaller than the entire site. P_{leave} is sampled every 20 time steps. When in state $\mathcal{L}$, a robot leaves the aggregation site by moving forward while avoiding collisions with other robots until it no longer perceives the site. At this point, the robot transitions from state $\mathcal{L}$ to state $\mathcal{RW}$. While on an aggregation site, *informed* robots count themselves in order to estimate n and x.

To model this scenario, we use ARGoS multi engine simulator [26]. The simulation environment models the circular arena as detailed above, and the kinematic and sensors readings of the Foot-bots mobile robots [27]. The robot sensory apparatus includes the proximity sensors positioned around the robot circular body, four ground sensors positioned two on the front and two on the back of the robot underside, and the range and bearing sensor. The proximity sensors are used for sensing and avoiding the walls of the arena. The readings of each ground sensors is set to 0.5 if the sensor is on grey, to 1 if on white, and 0 if on black. A robot perceives an aggregation site when all the four ground sensors return a value different from 0.5. The range and bearing sensor is used to avoid collision with other robots and to estimate how many *informed* robots are resting on a site within sensor range (i.e., the parameters n and x in eq. 2). With this sensor, two robots can perceive each other up to a distance of 0.8 meter.

3 Results with simulated robots

We run two sets of experiments (hereafter, setup 1, and setup 2), in which we varied the swarm size N, with $N = 50$ in setup 1, and $N = 100$ in setup 2. As aggregation performance are heavily influenced by swarm density [24, 9–11] in this paper we have decided to study scalability by keeping the swarm density constant. Therefore, the diameter of the area, as well as the diameters of the two sites, is varied as well (see Table 1). In both setups, the diameter of each aggregation site is large enough to accommodate all the robots of the swarm. Each setup

Table 1. Table showing the characteristics of each experimental condition in simulation

setup	swarm size	arena diameter	aggregation site diameter
1	50	12.9	2.8
2	100	19.2	4.0

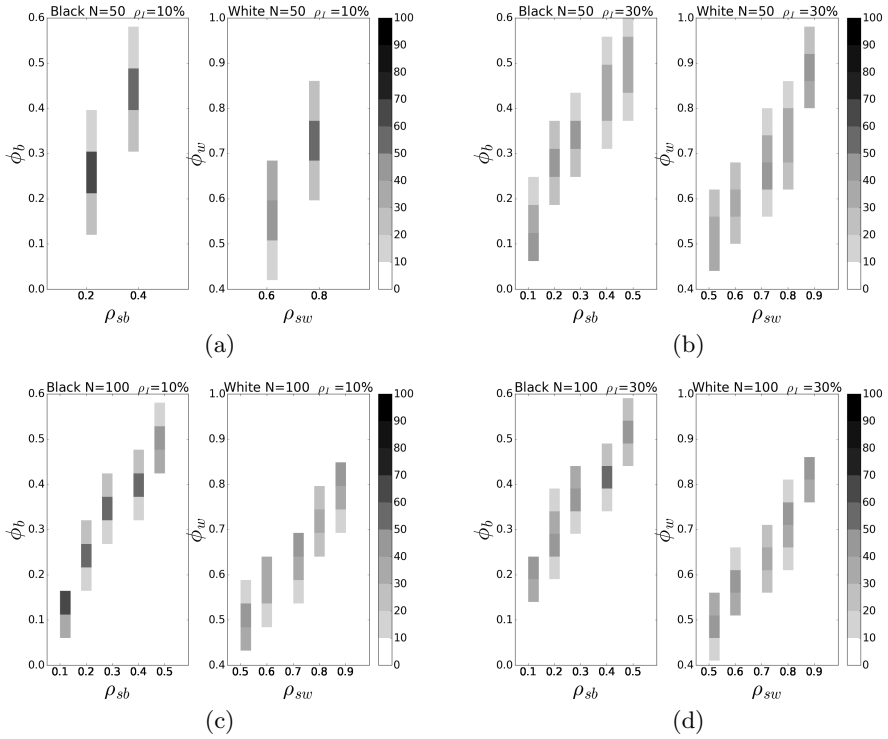

Fig. 2. Graphs in which the intensity of grey refers to the number of trials, out of 100, terminated with a particular proportion of robots on each site (i.e., Φ_b and Φ_w). The x-axes refer to the proportion of *informed* robots for black (ρ_{sb}) or for white (ρ_{sw}). The swarm size N and the total proportion of *informed* robots (ρ_I) in the swarm are: (a) $N = 50$ and $\rho_I = 0.1$; (b) $N = 50$ and $\rho_I = 0.3$; (c) $N = 100$ and $\rho_I = 0.1$; (d) $N = 100$ and $\rho_I = 0.3$. In each of these cases, the x and y-axis of the rightmost graphs refer to ρ_{sb} and Φ_b, respectively; the x and y-axis of the leftmost graphs refer to ρ_{sw} and Φ_w, respectively.

is made of 25 conditions which differ in the total proportion of *informed* robots in the swarm (hereafter, referred to as ρ_I, with $\rho_I = \{0.1, 0.3, 0.5, 0.7, 0.9\}$), and in the proportion of ρ_I that are informed for black (hereafter, referred to as ρ_{sb}, with $\rho_{sb} = \{0.1, 0.2, 0.3, 0.4, 0.5\}$) and for white (hereafter, referred to as ρ_{sw}, with $\rho_{sw} = 1 - \rho_{sb}$). For each condition, we execute 100 independent simulation trials. In each trial, the robots are randomly initialised within the arena. They autonomously move according to actions determined by their PFSM illustrated in Figure 1b for 300.000 time steps. One simulated second corresponds to 10 simulation time steps.

We expect that, for any value of ρ_I, the swarm distributes on each aggregation site in proportions that reflect the relative proportion of ρ_{sb} with respect to ρ_{sw}.

For example, for a given ρ_I, if $\rho_{sb} = 0.1$ and $\rho_{sw} = 0.9$, 10% of the swarm is expected to aggregate on the black site and the remaining 90% of the swarm is expected to aggregate on the white site. To evaluate the behaviour of the swarm we recorded the proportion of robots aggregated on the black site ($\Phi_b = \frac{N_b}{N}$) and on the white site ($\Phi_w = \frac{N_w}{N}$), at the end of each simulation run (where N_b and N_w are the number of robots aggregated on the black and white site, respectively, and N is the swarm size). In this paper, we show only the results of setup 1 and 2 relative to those conditions in which $\rho_I = 0.1, 0.3$ The results of these simulations are shown in Figure 2. Each graph shows the number of trials, out of 100, terminated with a particular proportion of robots i) on the black site, for each value of ρ_{sb} indicated on the x-axes of the rightmost graph in Figure 2a, 2b, 2c, and 2d; ii) on the white site, for each value of ρ_{sw} indicated on the x-axes of the leftmost graph in Figure 2a, 2b, 2c, and 2d. The swarm size N and the total proportion of *informed* robots (ρ_I) in the swarm are: i) $N = 50$ and $\rho_I = 0.1$ in Figure 2a; ii) $N = 50$ and $\rho_I = 0.3$ in Figure 2b; iii) $N = 100$ and $\rho_I = 0.1$ in Figure 2c; iv) $N = 100$ and $\rho_I = 0.3$ in Figure 2d.

Ideally, if the swarm aggregates in way to perfectly reflect the relative proportion of *informed* robots for black and for white in the swarm, for both $N = 50$ and $N = 100$ and for all total proportion of *informed* robots in the swarm, the graphs in Figure 2 would show only black rectangle aligned on the diagonal from bottom left to top right corners of each graph. In other words, all 100 trials in each condition of each setup would terminate with $\Phi_b = \rho_{sb}$ and $\Phi_w = \rho_{sw}$. The results of the simulations tend to slightly diverge from this ideal case. However, we can clearly see that a higher concentration of trials (the darker rectangles for each case) tend to be aligned on the above mentioned diagonal, with deviations from the ideal case that remain nevertheless close to the expected result. This is clearly observable even when the total proportion of informed robots is 0.1 of N for both setup1 with $N = 50$ and setup 2 with $N = 100$ (see Figure 2a and 2c, respectively). Note that the results in Figure 2 refer to the two most challenging scenarios, in which the total proportion of *informed* robots in the swarm is relatively low ($\rho_I = 0.1$ and $\rho_I = 0.3$). For higher proportion of *informed* robots in the swarm, the results of the simulations tend to get progressively closer to the best-case scenario, in which simulation trials terminates with $\Phi_b = \rho_{sb}$ and $\Phi_w = \rho_{sw}$.

In summary, the PFSM described in Section2 allows to rather accurately control the way in which the robots of a swarm distribute on two different aggregation sites simply by regulating the relative proportion of *informed* robots for each site, even with a small total proportion of *informed* robots in the swarm ($\rho_I = 0.1$), and for different swarm sizes.

4 Experiments with physical robots

In order to test the performances illustrated in Section 3 on physical robots, we run a further set of experiments with physical kilobot robots. A Kilobot is a small (33 mm diameter, 34 mm height), and low-cost robot developed at Har-

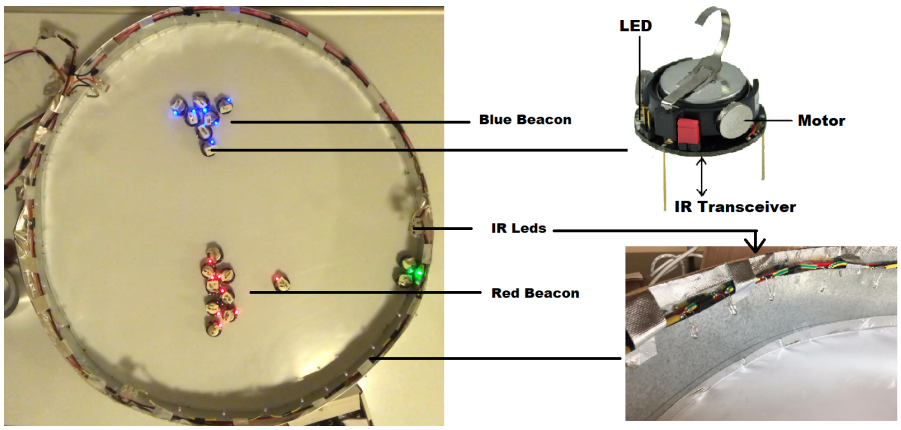

Fig. 3. The kilobots' arena with the aggregation sites represented by two kilobot beacons emitting red and blue light respectively. In the picture, the robots have their LED on emitting the light corresponding to the site in which they are currently resting. Since the robots do not use vision, LEDs are just for visualisation purpose. On the external side of the arena wall, infra-red emitters signal to the robots the arena's edges.

vard University, explicitly designed to run swarm robotics experiments [28]. The kilobot is equipped with infrared transceivers for communication and perception of other robots, as well as with an ambient light sensor and a coloured LED. Our physical robots scenario is made of a circular arena (80 cm diameter). On the external side of the arena wall, infra-red emitters, controlled by an Arduino micro-controller, signal to the robots the arena's edges, as illustrated in Figure 3. Each kilobot can perceive these infra-red signals from a distance of $8-10$ cm. These signals are used by the robots to avoid the arena walls during random walk. Two kilobots, positioned at approximately 40 cm from each other, at equal distance from the arena centre, represent the aggregation sites. These kilobots, referred to as beacons, have their LEDs emitting different colours: one emits blue light, and the other emits red light. In analogy with the simulation environment, the blue LED represents the black aggregation site, and the red LED the white site. The beacons communicate their position to the other robots using the infra-red transceivers, which have a range of $9-10$ cm. The kilobots use the infra-red transceivers also for estimating the parameters n and x of eq. 2. Each type of robot is controlled by the PFSM illustrated in Section 2. The only difference between simulated and physical robots is that for kilobot the parameter a in eq. 2 is set to $a = 3.6$, and P_{leave} is sampled every 10 sec.

The experimental design with physical robots slightly differs to the tests in simulations. This is due to the fact that the time required to execute a single trial with physical robots is significantly longer than the single trial in simulation. Thus, we have reduced the conditions under which the robotic system is tested. Moreover, the parameters ρ_I, ρ_{sb} and ρ_{sw} has been chosen by taking into account

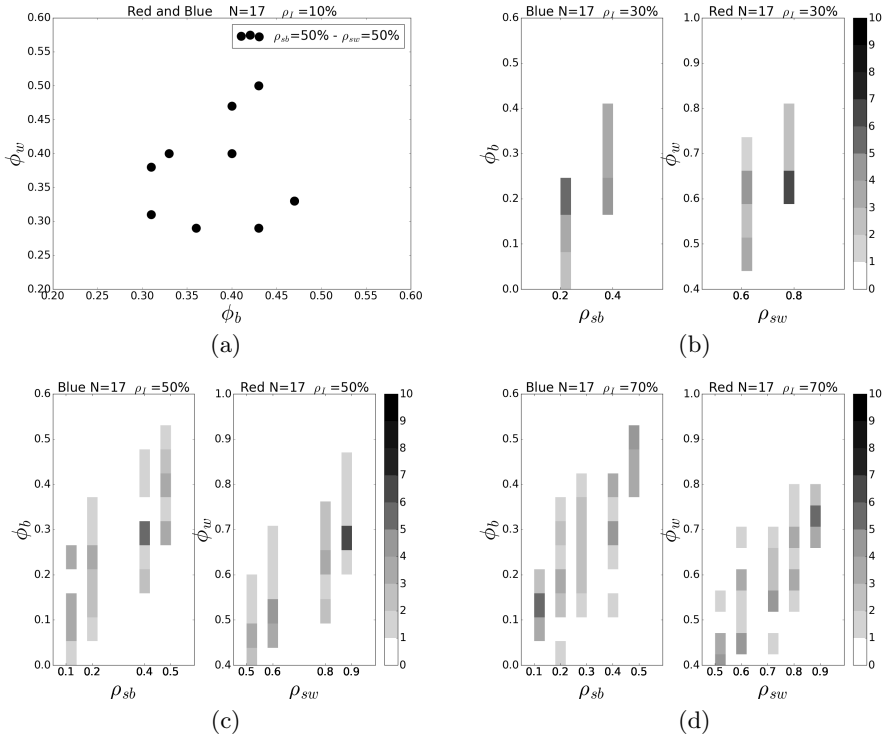

Fig. 4. (a) Scatter plot showing the proportion of robots aggregated on each site for $\rho_I = 0.1$, and $\rho_{sw} = \rho_{sb} = 0.5$. In (b), (c), and (d) the intensity of grey in each graph refers to the number of trials, out of 10, terminated with a particular proportion of robots on each site (i.e., Φ_b and Φ_w). The x and y-axis of the rightmost graphs refer to ρ_{sb} and Φ_b, respectively; the x and y-axis of the leftmost graphs refer to ρ_{sw} and Φ_w, respectively. $N = 17$ in all graphs.

the fact that we have at our disposal only 17 kilobots robots. Thus, we decided to test the following scenarios:

- for $\rho_I = 0.1$, we only tested the condition with $\rho_{sw} = \rho_{sb} = 0.5$;
- for $\rho_I = 0.3$, we tested the condition with $\rho_{sb} = 0.2$ and $\rho_{sw} = 0.8$, and the condition with $\rho_{sb} = 0.4$ and $\rho_{sw} = 0.6$;
- for $\rho_I = 0.5$, we tested the conditions with $\rho_{sb} = \{0.1, 0.2, 0.4, 0.5\}$ and $\rho_{sw} = 1 - \rho_{sb}$;
- for $\rho_I = 0.7$, we tested the conditions with $\rho_{sb} = \{0.1, 0.2, 0.3, 0.4, 0.5\}$ and $\rho_{sw} = 1 - \rho_{sb}$;

For each of the above mentioned conditions, we executed 10 trials. In each trial, the robots are initially placed within the arena in a pseudo-random way. During each trial, each robot is controlled by the PFSM described in Figure 1b. A

trial is ended according to the following criteria: 1) as soon as at least 80% of the kilobots are resting in any of the aggregation sites; or after 40 minutes if criterium 1 is never reached.

The results of our tests with physical kilobot robots are shows in Figure 4. The graph in Figure 4a refers to the most challenging scenario in which the proportion of *informed* robots is at its minimum (i.e., $\rho_I = 0.1$). In this condition, we explore only the case for $\rho_{sb} = \rho_{sw}$. Contrary to simulations, *informed* robots has only a marginal influence on the aggregation dynamics. Both Φ_b and Φ_w tend to be smaller than the expected outcomes that, for this conditions, correspond to half of the kilobots on the black and half of them on the white site. The differences in results between the physical and simulated robots in the same condition (i.e., $\rho_I = 0.1$, $\rho_b = \rho_w = 0.5$) could be an effect of the swarm size with physical robots, which is significantly smaller than the swarm size with simulated robots. In all the other conditions (see Figure 4b, 4c, 4d), the physical robots tend to generate better results. We clearly notice that there is a strong correlation between how we vary ρ_{sb} and ρ_{sw} and the resulting Φ_b and Φ_w. However, also for all these conditions, the relatively small swarm size seems to have a negative effect on the possibility of *informed* robots to control the aggregation dynamics. Moreover, we observed that collisions with the arena wall from specific orientation very often resulted in deadlocks from which the robots could not recover. This has certainly contributed to lower the proportion of robots that manage to reach and rest on each aggregation site. In summary, we believe that, in spite of the disruptive effects caused by the small swarm size and by the collisions between the robots and the arena wall, the results shown in Figure 4 validate our approach in which the relative proportion of different types of *informed* robots is used to control the aggregation dynamics of a swarm of heterogeneous robots.

5 Conclusions

In this paper, we have shown that the aggregation dynamics of a swarm of robots can be controlled using the system heterogeneity. In this self-organised aggregation scenario, with a swarm of robots required to operate in an arena with two aggregation sites, the system heterogeneity is represented by *informed* robots; that is, agents that selectively avoid a type of aggregation site (i.e., the black/white site) to systematically rest on the other type of site (i.e., the white/black site). The results of our simulations indicate that with a small proportion of *informed* robots a designer can effectively control the way in which an entire swarm distribute on the two aggregation sites. This is because the size of the robots' aggregates at each site tends to match the relative proportion of the two different types of *informed* robots characterising the swarm. The results of the simulations have been validated by a set of experiments with physical kilobot robots. Nevertheless, the behaviour of the physical robots has been negatively affected by the frequent collisions between the robots and the arena wall which, relatively often, represented deadlock conditions with the robots unable

to generate the virtuous manoeuvres necessary to recover movement. We also believe that the small size of the physical robots swarm has contributed to limit the influential role of *informed* robots. However, further studies are required to better characterise the nature of the relationship between the swarm size and the aggregation mechanisms we have discussed in this paper.

We believe that the system heterogeneity, relatively neglected in swarm robotics, can play an important role in the development of mechanisms to control the self-organised collective responses of swarms of robots. Our research agenda for the future is focused on the series of experiments based on the hypothesis that the system heterogeneity has a measurable impact on the outcomes of certain self-organised processes. We aim to identify these processes and to illustrate how they can be effectively controlled by manipulating the system heterogeneity.

References

1. M. Brambilla, E. Ferrante, M. Birattari, and M. Dorigo, "Swarm robotics: a review from the swarm engineering perspective," *Swarm Intelligence*, vol. 7, no. 1, pp. 1–41, 2013.
2. E. Bonabeau, M. Dorigo, D. d. R. D. F. Marco, G. Theraulaz, *et al.*, *Swarm intelligence: from natural to artificial systems*. Oxford university press, 1999.
3. G. Valentini, E. Ferrante, and M. Dorigo, "The best-of-n problem in robot swarms: Formalization, state of the art, and novel perspectives," *Frontiers in Robotics and AI*, vol. 4, p. 9, 2017.
4. G. Valentini, E. Ferrante, H. Hamann, and M. Dorigo, "Collective decision with 100 Kilobots: Speed versus accuracy in binary discrimination problems," *Autonomous Agents and Multi-Agent Systems*, vol. 30, no. 3, pp. 553–580, 2016.
5. I. Couzin, J. Krause, N. Franks, and S. Levin, "Effective leadership and decision making in animal groups on the move," *Nature*, vol. 433, pp. 513–516, 2005.
6. H. Çelikkanat and E. Şahin, "Steering self-organized robot flocks through externally guided individuals," *Neural Computing and Applications*, vol. 19, pp. 849–865, Sep 2010.
7. E. Ferrante, A. E. Turgut, C. Huepe, A. Stranieri, C. Pinciroli, and M. Dorigo, "Self-organized flocking with a mobile robot swarm: a novel motion control method," *Adaptive Behavior*, vol. 20, no. 6, pp. 460–477, 2012.
8. E. Ferrante, A. Turgut, A. Stranieri, C. Pinciroli, M. Birattari, and M. Dorigo, "A self-adaptive communication strategy for flocking in stationary and non-stationary environments," *Natural Computing*, vol. 13, no. 2, pp. 225–245, 2014.
9. Z. Firat, E. Ferrante, N. Cambier, and E. Tuci, "Self-organised aggregation in swarms of robots with informed robots," in *International Conference on Theory and Practice of Natural Computing*, pp. 49–60, Springer, 2018.
10. Z. Firat, E. Ferrante, Y. Gillet, and E. Tuci, "On self-organised aggregation dynamics in swarms of robots with informed robots," *Neural Computing and Applications*, pp. 1–17, 2020.
11. Y. Gillet, E. Ferrante, Z. Firat, and E. Tuci, "Guiding aggregation dynamics in a swarm of agents via informed individuals: an analytical study," in *The 2018 Conference on Artificial Life: A Hybrid of the European Conference on Artificial Life (ECAL) and the International Conference on the Synthesis and Simulation of Living Systems (ALIFE)*, pp. 590–597, MIT Press, 2019.

12. N. Correll and A. Martinoli, "Modeling and designing self-organized aggregation in a swarm of miniature robots," *The International Journal of Robotics Research*, vol. 30, no. 5, pp. 615 – 626, 2011.
13. M. Gauci, J. Chen, W. Li, T. Dodd, and R. Groß, "Self-organized aggregation without computation," *The International Journal of Robotics Research*, vol. 33, no. 8, pp. 1145–1161, 2014.
14. L. Bayindir and E. Şahin, "Modeling self-organized aggregation in swarm robotic systems," in *IEEE Swarm Intelligence Symposium, SIS'09*, pp. 88–95, IEEE, 2009.
15. J. Deneubourg, A. Lioni, and C. Detrain, "Dynamics of aggregation and emergence of cooperation," *The Biological Bulletin*, vol. 202, no. 3, pp. 262–267, 2002.
16. R. Jeanson, C. Rivault, J. Deneubourg, S. Blanco, R. Fournier, C. Jost, and G. Theraulaz, "Self-organized aggregation in cockroaches," *Animal Behaviour*, vol. 69, no. 1, pp. 169–180, 2005.
17. S. Garnier, C. Jost, R. Jeanson, J. Gautrais, M. Asadpour, G. Caprari, and G. Theraulaz, "Aggregation behaviour as a source of collective decision in a group of cockroach-like-robots," in *European Conference on Artificial Life*, pp. 169–178, Springer, 2005.
18. S. Garnier, C. Jost, J. Gautrais, M. Asadpour, G. Caprari, R. Jeanson, A. Grimal, and G. Theraulaz, "The embodiment of cockroach aggregation behavior in a group of micro-robots," *Artificial life*, vol. 14, no. 4, pp. 387–408, 2008.
19. M. Dorigo, V. Trianni, E. Şahin, R. Groß, T. Labella, G. Baldassarre, S. Nolfi, J. Deneubourg, F. Mondada, D. Floreano, *et al.*, "Evolving self-organizing behaviors for a swarm-bot," *Autonomous Robots*, vol. 17, no. 2, pp. 223–245, 2004.
20. E. Tuci, M. Alkilabi, and O. Akanyety, "Cooperative object transport in multi-robot systems: A review of the state-of-the-art," *Frontiers in Robotics and AI*, vol. 5, pp. 1–15, 2018.
21. N. Cambier, V. Frémont, V. Trianni, and E. Ferrante, "Embodied evolution of self-organised aggregation by cultural propagation," in *ANTS 2018*, (Rome, Italy), 2018.
22. S. Garnier, J. Gautrais, M. Asadpour, C. Jost, and G. Theraulaz, "Self-organized aggregation triggers collective decision making in a group of cockroach-like robots," *Adaptive Behavior*, vol. 17, no. 2, pp. 109–133, 2009.
23. A. Campo, S. Garnier, O. Dédriche, M. Zekkri, and M. Dorigo, "Self-organized discrimination of resources," *PLoS ONE*, vol. 6, no. 5, p. e19888, 2010.
24. N. Cambier, V. Fremont, V. Trianni, and E. Ferrante, "Embodied evolution of self-organised aggregation by cultural propagation," in *Proc. of the* 11^{th} *Int. Conf. on Swarm Intelligence* (M. D. et al., ed.), LNCS, p. In Press, Springer, 2018.
25. S. Kato and M. Jones, "An extended family of circular distributions related to wrapped cauchy distributions via brownian motion," *Bernoulli*, vol. 19, no. 1, pp. 154–171, 2013.
26. C. Pinciroli, V. Trianni, R. O'Grady, G. Pini, A. Brutschy, M. Brambilla, N. Mathews, E. Ferrante, G. Di Caro, F. Ducatelle, M. Birattari, L. Gambardella, and M. Dorigo, "ARGoS: a modular, parallel, multi-engine simulator for multi-robot systems," *Swarm Intelligence*, vol. 6, no. 4, pp. 271–295, 2012.
27. M. Bonani, V. Longchamp, S. Magnenat, P. Rétornaz, D. Burnier, G. Roulet, F. Vaussard, H. Bleuler, and F. Mondada, "The marxbot, a miniature mobile robot opening new perspectives for the collective-robotic research," in *IEEE/RSJ Int. Conf. on Intelligent Robots and Systems (IROS)*, pp. 4187–4193, 2010.
28. M. Rubenstein, C. Ahler, N. Hoff, A. Cabrera, and R. Nagpal, "Kilobot: A low cost robot with scalable operations designed for collective behaviors," *Robotics and Autonomous Systems*, vol. 62, no. 7, pp. 966–975, 2014.